

Adapting algebraic diagrammatic construction schemes for the polarization propagator to problems with multi-reference electronic ground states exploiting the spin-flip *ansatz*

Cite as: J. Chem. Phys. **143**, 124107 (2015); <https://doi.org/10.1063/1.4931653>

Submitted: 29 November 2014 . Accepted: 13 September 2015 . Published Online: 28 September 2015

Daniel Lefrancois, Michael Wormit, and Andreas Dreuw



View Online



Export Citation



CrossMark

ARTICLES YOU MAY BE INTERESTED IN

[The third-order algebraic diagrammatic construction method \(ADC\(3\)\) for the polarization propagator for closed-shell molecules: Efficient implementation and benchmarking](#)

The Journal of Chemical Physics **141**, 064113 (2014); <https://doi.org/10.1063/1.4892418>

[Analysis and comparison of CVS-ADC approaches up to third order for the calculation of core-excited states](#)

The Journal of Chemical Physics **142**, 214104 (2015); <https://doi.org/10.1063/1.4921841>

[Accurate adiabatic singlet-triplet gaps in atoms and molecules employing the third-order spin-flip algebraic diagrammatic construction scheme for the polarization propagator](#)

The Journal of Chemical Physics **145**, 084102 (2016); <https://doi.org/10.1063/1.4961298>



Your Qubits. Measured.

Meet the next generation of quantum analyzers

- Readout for up to 64 qubits
- Operation at up to 8.5 GHz, mixer-calibration-free
- Signal optimization with minimal latency

Find out more



Adapting algebraic diagrammatic construction schemes for the polarization propagator to problems with multi-reference electronic ground states exploiting the spin-flip *ansatz*

Daniel Lefrancois, Michael Wormit, and Andreas Dreuw^{a)}

Interdisciplinary Center for Scientific Computing, Ruprecht-Karls University, Im Neuenheimer Feld 368, 69120 Heidelberg, Germany

(Received 29 November 2014; accepted 13 September 2015; published online 28 September 2015)

For the investigation of molecular systems with electronic ground states exhibiting multi-reference character, a spin-flip (SF) version of the algebraic diagrammatic construction (ADC) scheme for the polarization propagator up to third order perturbation theory (SF-ADC(3)) is derived via the intermediate state representation and implemented into our existing ADC computer program *adcm*. The accuracy of these new SF-ADC(*n*) approaches is tested on typical situations, in which the ground state acquires multi-reference character, like bond breaking of H₂ and HF, the torsional motion of ethylene, and the excited states of rectangular and square-planar cyclobutadiene. Overall, the results of SF-ADC(*n*) reveal an accurate description of these systems in comparison with standard multi-reference methods. Thus, the spin-flip versions of ADC are easy-to-use methods for the calculation of “few-reference” systems, which possess a stable single-reference triplet ground state. © 2015 AIP Publishing LLC. [<http://dx.doi.org/10.1063/1.4931653>]

I. INTRODUCTION

In principle, stable organic molecules, which can be put in a flask and stored for years without degradation, possess a closed-shell electronic ground state, which is usually energetically well separated from other electronic states. As a consequence, the Born-Oppenheimer approximation holds and the ground-state wavefunction is well described with a single Slater determinant capturing up to 95% of the total energy.^{1,2} For such molecules, single-reference electron correlation methods like Møller-Plesset perturbation theory or standard coupled-cluster methods are well suited for the calculation of energies, molecular properties, and spectra.^{3,4} Most of chemistry, however, focuses on molecular reactions, in which chemical bonds are broken and formed, which naturally leads to substantial multi-reference character of the ground state electronic wavefunction. The theoretical description of bond-breaking thus requires a consistent description of a well-defined single-reference wavefunction at the equilibrium distance and of multi-reference situations at bond dissociation.

The typical quantum chemical methods of choice for the computation of multi-reference situations like bond-breaking are, for instance, complete and restricted active space self-consistent field (CASSCF and RASSCF),^{5–8} which are often augmented with a perturbation theoretical treatment of second order to capture the missing dynamical correlation, as, for example, in CASPT2.^{9,10} Also, multi-reference configuration interaction (MRCI) and coupled-cluster (MRCC) based methods^{11–13} are developed and successfully employed for the investigation of molecules with pronounced multi-reference character. Different MRCI programs are nowadays available which make use of different references, e.g., standard Hartree-

Fock references,^{14–16} semi-empirical references stemming, for example, from the Austin model 1 (AM1)^{17–19} or the orthogonalization method 2 (OM2),^{19,20} or from density-functional theory (DFT) as in DFT/MRCI.^{21,22} The latter are particularly well suited to study medium-sized to large molecular systems. In general, the application of active-space and multi-reference methods requires *a priori* knowledge of the chemical system under investigation since molecular orbitals and configuration spaces need to be chosen.

Interesting alternatives to these methods with multi-reference ground-state treatment are offered by the so-called spin-flip (SF) approaches.²³ The key idea of SF is to choose the triplet ground-state as a reference and to calculate a multi-reference singlet ground-state as “excitation,” in which the spin of the excited electron is flipped, using standard single-reference methodologies. In single bond-breaking, for example, the singlet ground-state usually requires two leading references for its physically correct theoretical description, while for the triplet ground-state, a single reference is often enough along the complete dissociation pathway. It is worth to note that triplets often exhibit single-reference character as long as the corresponding singlet ground state comprises only a few leading reference states. It is clear that as soon as the triplet ground state acquires itself multi-reference character, simple SF approaches are no longer applicable. Due to this limitation of SF approaches, we prefer to call single SF approaches rather “few-reference” instead of “multi-reference” methods. In principle, the spin-flip concept is conceptually easily extendable to double, triple, etc., spin-flip excitations; however, only double spin flip has been realized so far and only little is known about its performance.²⁴

Until today, the SF idea has been successfully exploited to derive, for example, equation-of motion spin-flip coupled-cluster (EOM-SF-CC),²³ spin-flip density functional theory

^{a)}Electronic mail: dreuw@uni-heidelberg.de

(SF-DFT),^{25–27} and spin-flip configuration interaction (SF-CI) methods.^{28–30} Of course, these spin-flip methods inherit the properties of their parent nonspin-flip approaches. As a consequence, SF-DFT has conceptual problems with charge transfer states³¹ when standard exchange-correlation functionals are employed. SF-CC approaches are non-Hermitian methods, and hence, the rigorous calculation of properties is in general cumbersome.^{32,33} Furthermore, the computational effort of SF approaches is the same as for the parent method, e.g., SF-DFT like regular unrestricted DFT, SF-algebraic diagrammatic construction (SF-ADC) like unrestricted ADC and SF-CC approaches like their standard unrestricted counterparts. Highly accurate calculations at, for example, EOM-SF-CC with singles, doubles, and triples excitations (EOM-SF-CCSDT) or, if available, ADC(4) are typically not feasible for medium and large molecules owing to the steep scaling of its computational effort with system size in the order of $O(N^8)$ with N being the number of one-particle basis functions.

Nevertheless, typical few-reference problems have been studied successfully employing spin-flip approaches demonstrating the potential of this conceptually simple *ansatz*. These comprise bond-breaking of, for example, diatomic molecules like H_2 and HF ^{23,28,29,34,35} or the torsional motion of ethylene through a well-known conical intersection.^{23,28,29,34–37} Further examples are the excitation energies of the beryllium atom,^{23,28,29} bi- and triradicals such as trimethylenemethane,^{28,29,37} cyclobutadiene (CBD),^{38,39} and 5-dehydro-m-xylylene.³⁷ Several molecules such as methylene (CH_2),³⁴ the amidogen ion (NH_2^+),³⁸ oxygen (O_2),³⁴ and ozone (O_3)³⁴ also exhibit strong multi-reference ground state wave function due to the highly diradicaloid character. CBD, in particular, is a famous example for a molecule with a multi-reference ground state wavefunction, and using single-reference methods for its description, a large spin-contamination is noticeable, i.e., a large deviation from the correct expectation value of the \hat{S}^2 operator of zero. Substantial spin contamination is a typical observation for multi-reference systems when single-reference methods are employed.³⁵ The electronic ground and excited states of CBD have thus served previously as a testing ground for spin-flip methods.^{23,25–30}

The ADC schemes for the polarization propagator have recently shown to represent a valuable alternative to EOM-CC and linear-response CC (LR-CC) approaches.^{40–45} Hence, SF-ADC should be an equally valuable alternative to SF-CC approaches. As in all other ADC methods, the algebraic SF-ADC equation is a Hermitian eigenvalue problem, directly affording excitation energies as eigenvalues and transition amplitudes as eigenvectors in the intermediate state basis. Due to its Hermitian structure, the calculation of excited state properties is conceptually simple. Since the multi-reference singlet ground state is obtained as “excited state” of the triplet ground state, also properties of the singlet ground state are easily accessible with SF-ADC. In addition, energies and properties computed with ADC are fully size-consistent.

In this paper, we present the first realization of SF-ADC for excitation energies up to third order of perturbation theory using unrestricted and restricted open-shell ground state triplet references. In Section II, the theoretical background and implementation of SF-ADC are outlined. The results of initial

tests of SF-ADC are described in Section III, in which the breaking of single bonds, twisting of double bonds, and the excited states of CBD are investigated. The paper concludes with a brief summary of the main results (Section IV).

II. THEORY AND IMPLEMENTATION OF SF-ADC

While, historically, ADC has been derived via diagrammatic perturbation theory for the polarization propagator^{40,41} using the partitioning of the Hamiltonian according to Møller and Plesset, algebraic expressions for ADC schemes can nowadays be derived elegantly via the so-called intermediate-state representation (ISR) formalism resulting in so-called non-Dyson ISR-ADC schemes.⁴³ Following this route, unrestricted versions of ADC (UADC(n)) have already been derived and implemented⁴⁶ as well as relativistic four-component ADC schemes for the polarization propagator.⁴⁷ In addition, the route via the intermediate state representation gives access to excited state wavefunctions and allows thus for an efficient computation of excited state and state-to-state transition properties.^{42,43} To understand the key difference between standard non-SF-ADC schemes and SF-ADC, a brief account of the derivation via the ISR shall be given.

The ISs represent the orthonormal basis $\{\tilde{\Psi}_J\}$, in which the algebraic expressions of the ADC equation are given

$$\mathbf{M}\mathbf{X} = \Omega\mathbf{X}, \quad \mathbf{X}^\dagger\mathbf{X} = 1, \quad (1)$$

or in other words, the IS is the basis, in which the Hamiltonian shifted by the ground-state energy is represented as

$$M_{JJ} = \langle \tilde{\Psi}_J | \mathcal{H} - E_0 | \tilde{\Psi}_J \rangle. \quad (2)$$

In this representation, the coupling between the exact ground state and the orthogonal excited states via the Hamiltonian vanishes. Hence, it is clear that diagonalization of \mathbf{M} , i.e., solution of Eq. (1) yields excitation energies ω_n and ADC vectors \mathbf{X}_n of the transition amplitudes. The ADC vectors do not correspond to the excited state wavefunctions $|\Psi_n\rangle$, since the latter are given by

$$|\Psi_n\rangle = \sum_J X_{Jn} |\tilde{\Psi}_J\rangle. \quad (3)$$

The key to the derivation of different ADC schemes lies in the construction of the IS basis functions. In a first step, a non-orthogonal set of correlated excited states is constructed by acting with physical excitation operators on an appropriate Møller-Plesset ground state wavefunction according to

$$|\Psi_J^0\rangle = \hat{C}_J |\Psi_0^{MPn}\rangle, \quad (4)$$

where the excitation operators are defined as

$$\{\hat{C}_J\} = \{c_{a\sigma}^\dagger c_{i\sigma}; c_{a\sigma}^\dagger c_{b\tau}^\dagger c_{i\sigma} c_{j\tau}; \dots\}, \quad (5)$$

yielding singly excited, so-called particle-hole (p-h) states, doubly excited, so-called two-particle-two-hole (2p-2h) states, and so on. The one-particle states (spin orbitals) $|\phi_{p\sigma}\rangle$ are denoted with indices a, b, c for unoccupied (virtual) and i, j, k for occupied orbitals. Subsequent orthogonalization of these states via Gram-Schmidt yields the intermediate state basis $\{\tilde{\Psi}_J\}$ needed to set up the corresponding ADC matrix according to Eq. (2).

If, for example, in the course of the derivation, the second-order Møller-Plesset ground state wavefunction and energy are chosen to construct the IS basis and to shift the electronic Hamiltonian according to Eqs. (4) and (2), the strict second-order ADC scheme ADC(2)-s is obtained. Since the MP2 ground state energy includes nothing but all contributions up to second order while the excitation energies for the primary p-h states contain all second order terms but also contributions of higher order, the combination of the MP2 ground state energy and the ADC(2)-s excitation energies to obtain potential energy surfaces seems not well defined from a perturbation theoretical point of view. However, following the derivation of ADC approaches via the ISR formalism as outlined above, the ADC matrix and the IS basis are *constructed* with respect to the MP2 ground state energy and wavefunction, respectively. It is also important to recognize that the couplings between the ground state MP wavefunction and the intermediate states vanish exactly order by order, i.e., in a consistent second-order scheme, all couplings up to second order are zero, and all higher-order terms are neglected. The same holds for the higher-order ADC(n) schemes and their relation to the corresponding MPn ground state. Since the corresponding MPn ground state has been chosen to construct the IS basis and their couplings vanish up to the respective order, the corresponding MPn energy is the natural choice for the calculation of total energies. In fact, the expression for the total energy of an excited state of ISR-derived ADC schemes has already been provided in Ref. 43. ADC(2)-x is not a consistent second order scheme, since the 2p2h block is *ad hoc* extended from 0th to 1st order as in ADC(3) to improve the description of doubly excited states leading to a pronounced unbalanced treatment of the ground and excited states. Nevertheless, the MP2 ground state energy is also here chosen, which leads to a systematic underestimation of excitation energies.⁴⁵

Until today, the ISR formalism using the MPn energy or wavefunction as a reference for the computation of excited state energies and excited-state properties via ADC(n) has been employed to investigate, for example, static excited state dipole moments and excited state geometries.^{43,48} Here, the agreement between ADC schemes and full configuration interaction (FCI) has been found to be very satisfactory, in particular for HF.⁴³ Also, excited-state geometry optimizations at ADC(2) level, in which the gradient of the MP2 ground state energy is added to one of the ADC(2) excitation energies, yield accuracies similar to those at EOM-CCSD level.⁴⁸ At this point, however, it is also worthwhile to note that the description of contributions to the excited states originating from higher-order electronic ground state correlation can be generally improved via the so-called Dyson-expansion method;⁴⁹ however, a discussion of this procedure goes beyond the topic of the current work, but will be investigated in detail in the future.

Returning to the derivation of ADC schemes via the ISR formalism, the nature of the excitation operators chosen in Eq. (5) eventually determines the variant of the ADC scheme. For example, the singlet MP ground-state is used in non-SF-ADC schemes as reference and the excitation operators \hat{C}_J are restricted to $\Delta m_s = 0$ excitations to conserve the spin of the system. In contrast, in SF-ADC, the triplet ground state is

chosen as a reference and the excitation operators are restricted to perform a spin flip ($\Delta m_s = -1$) to generate all singlet states including the singlet ground state as well as all triplet states with $m_s = 0$ according to

$$\{\hat{C}_J\} = \{c_{a\beta}^\dagger c_{i\alpha}; c_{a\beta}^\dagger c_{b\sigma}^\dagger c_{i\alpha} c_{j\sigma}, \quad a < b, i < j\}. \quad (6)$$

It should be noticed that within the double excitations, only one spin is flipped, while the second excitation conserves the spin and follows the $\Delta m_s = 0$ rule. Using the resulting IS basis to represent the electronic Hamiltonian shifted by the ground state triplet MP energy readily yields algebraic expressions for SF-ADC schemes,

$$M^{SF}X = \Omega X, \quad X^\dagger X = 1. \quad (7)$$

Diagonalization of M^{SF} yields the excitation energies of the target states relative to the triplet ground state and the corresponding ADC transition vectors in the IS basis.⁵⁰ In analogy to non-SF-ADC schemes, the ADC vectors in combination with the IS basis give access to excited-state properties and state-to-state transition properties. It is important to realize that also the properties of the potentially multi-reference singlet ground state can now be computed following this route, as will be demonstrated below. In principle, the spin-flip concept is extendable to multiple spin flips such as double spin flip (2SF), which has already been realized for EOM-2SF-CC.²⁴

Starting from an existing unrestricted spin-orbital ADC code,⁴⁶ the realization of SF-ADC variants is straightforward due to the structure of the corresponding ADC matrix (Fig. 1). In Fig. 1, the ph-block of the UADC matrix is shown demonstrating that the spin-mixed blocks ($\alpha\beta$ and $\beta\alpha$) do neither couple to each other nor couple to the spin-pure blocks ($\alpha\alpha$ and $\beta\beta$). This uncoupled structure is indeed given for the complete ADC(2) and ADC(3) matrices. The computation of energies and eigenvectors for spin-flipped states is hence simple, since a guess vector needs just to be created, which is nonzero only in the relevant ($\alpha\beta$) block. Iterative diagonalization via a Davidson algorithm can then yield only spin-flipped states. No further changes need to be made to the original spin-orbital ADC matrix. These modifications have been included into our existing ADC computer program *adman*,⁴⁴ which is a part of a development version of the Q-Chem 4.2 program package,⁵¹

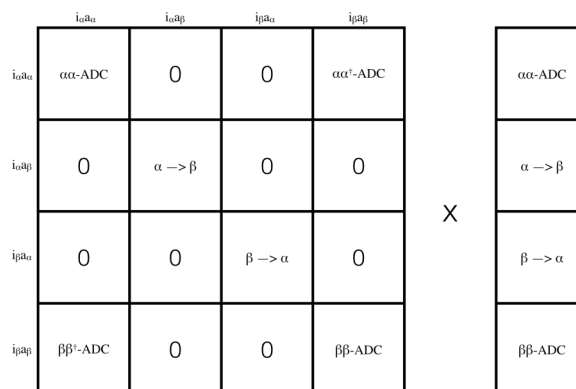


FIG. 1. Structure of the ph-block of the ADC matrix in for single ϕ_i^α excitation and guess vector.

which has been used for all numerical tests of the SF-ADC methods and the SF-EOM-CC calculations.

III. NUMERICAL TESTS OF SF-ADC

In this section, the performance of SF-ADC approaches in situations when the electronic ground state acquires multi-reference situations is tested against typical multi-reference methods. For that objective, we have chosen three prototypical examples: breaking of single bonds, twisting of double bonds, and the excited states of rectangular and square-planar diradicaloid cyclobutadiene. In these examples, the singlet ground state acquires multi-reference character with essentially two leading references, which we suggest to call “few-reference” situations. In most of such cases, the triplet ground state is well represented by a single reference determinant which can thus be used as input for a SF-ADC calculation. In addition, these determinants are usually not spin-contaminated. In all cases presented here, the S^2 expectation value of the unrestricted Hartree-Fock (UHF) reference varies between 2.00 and 2.02.

A. Breaking single bonds: H_2 and HF

The simplest numerical test of the capability of the SF-ADC approaches in describing the few-reference situation arising in breaking a covalent bond is to compute the potential energy curve (PEC) of the singlet ground state $^1\Sigma_g^+$ of the hydrogen molecule H_2 along the dissociation pathway. It is well known that Møller-Plesset perturbation theory in second and third orders, i.e., the ground state methods underlying the standard ADC schemes, is not capable of describing this dissociation. For illustration, the PEC of H_2 at the level of MP3/cc-pVTZ is shown in Fig. 2 in comparison to the numerically exact FCI/cc-pVTZ curve. The perturbation theoretical collapse of the MP3 approach beyond a bond length of 1.2 Å is readily apparent.

Going to spin flip ADC approaches, it can be seen that the strict spin-flip ADC(2) approach (SF-ADC(2)-s) lies on

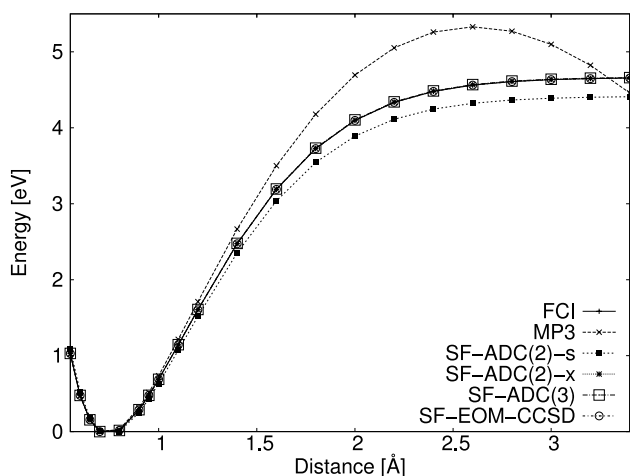


FIG. 2. Potential energy curves of the $^1\Sigma_g^+$ ground state of H_2 computed at the levels of full-CI, MP3, and various spin-flip ADC and EOM-CC methods. The energy at the equilibrium is set to zero.

top of the FCI curve in the vicinity of the minimum, i.e., below 1.1 Å. For larger bond distances, the ADC(2)-s curve starts to deviate from FCI, underestimating the dissociation energy in the dissociation limit by -0.25 eV. Nevertheless, the overall shape of the curve is qualitatively correctly reproduced, since SF-ADC(2)-s captures already the static correlation, but provides an incomplete description of the dynamic correlation of the two electrons. In contrast to SF-ADC(2)-s, the PECs obtained at SF-ADC(2)-x and SF-ADC(3) as well as SF-EOM-CCSD levels lie on top of the FCI curve, perfectly reproducing the static and dynamical electron correlations. This is of course due to the fact that the doubly excited states are completely included in these approaches allowing for a complete description of the electronic structure of H_2 .

Having analyzed the performance of SF-ADC approaches along the most simple bond dissociation of H_2 , let us turn to the slightly more complex case of the dissociation of the hydrogen fluoride (HF) molecule. The potential energy curves of HF have been calculated at the level of FCI/3-21G, which serve as benchmark for the other approaches. The calculations have been performed with the ORCA program package (version 2.9.1).⁵² In analogy to H_2 , MP3 can also not describe the dissociation of the HF bond in its $^1\Sigma^+$ ground state and the perturbational breakdown is readily apparent in Fig. 3 starting at a HF bond distance of about 1.4 Å.

All employed spin-flip ADC approaches as well as SF-EOM-CCSD give qualitatively correct shapes of the ground state $X^1\Sigma^+$ dissociation curve. However, the PEC computed at the SF-ADC(2)-s level deviates most strongly from the FCI reference. Starting at the equilibrium distance, the curve rises too steeply and then falls off too strongly cutting the FCI curve at a bond distance of 2 Å. Eventually, the asymptotic dissociation limit is underestimated by about -0.5 eV. SF-ADC(2)-x yields a PEC for the $X^1\Sigma^+$ state that agrees much better with the FCI curve than the one of SF-ADC(2)-s. Still, at the dissociation limit, SF-ADC(2)-x overestimates the dissociation energy by 0.2 eV. SF-ADC(3) describes the dissociation of HF in the ground state most accurately and lies practically on top of the FCI curve in the vicinity of the

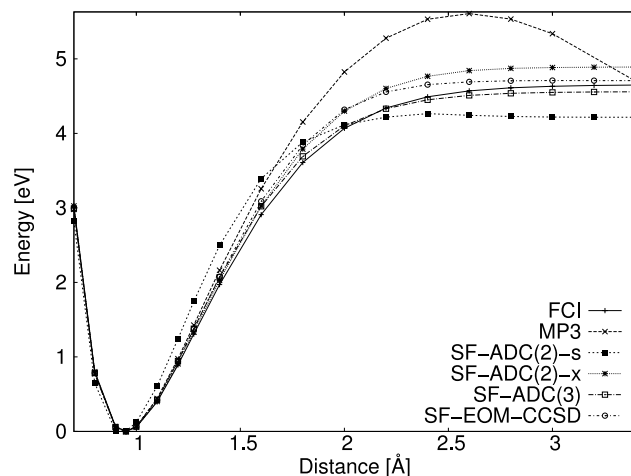


FIG. 3. Potential energy curves of the $X^1\Sigma^+$ ground state of HF computed at the levels of full-CI, MP3, and various spin-flip ADC and EOM-CC methods. The energy at the equilibrium is set to zero for all curves.

equilibrium distance (Fig. 3). Over the whole dissociation coordinate, it deviates by not more than 0.1 eV and underestimates the dissociation limit by -0.1 eV. In comparison, SF-EOM-CCSD deviates stronger in the intermediate bond length range and converges to a slightly overestimated dissociation energy by about 0.06 eV (Fig. 3). A recently well established measure for the analysis of the accuracy of potential energy curves is the non-parallelity error (NPE), which amounts to 39.2, 10.2, and 12.7 mhartree in the case of SF-ADC(2)-s, SF-ADC(2)-x, and SF-ADC(3), respectively, reaching an accuracy sufficient for a qualitative analysis in contrast to the standard ADC(3) method, which cannot be used at all to study single-bond breaking. Certainly, traditional multi-reference methods reach a much higher quantitative accuracy with NPEs of 1 mhartree or less.^{53–55} For example, state-specific MRCCSD calculations give NPEs as small as 1.9 mhartree⁵⁴ and the more recently developed internally contracted MRCCSD scheme even of only 0.11 mhartree⁵⁵ for the HF molecule. Various multireference perturbation theories including CASPT2, MK-MRPT2, NEVPT2, for instance, also yield PES with NPEs less than 7 mhartree.⁵⁶

At this point, it is instructive to compare the potential energy curves of the lowest-lying singlet states of hydrogen fluoride $X^1\Sigma^+$, $1^1\Pi$, and $2^1\Sigma^+$ computed at the FCI level with those obtained using SF-ADC(3) and conventional ADC(3) (Figure 4). All PECs of these states agree very well for bond distances below 1.3 Å, i.e., in the vicinity of the equilibrium structure. For bond distances larger than 1.3 Å, the PECs of the $X^1\Sigma^+$ and $B^1\Sigma^+$ states start to deviate substantially from the FCI curves at conventional ADC(3) level. However, the $1^1\Pi$ state remains reasonably well described up to a bond distance of 2.8 Å. The breakdown of conventional ADC(3) with increasing bond length is of course related to the failure of the underlying single-reference MP3 method in the description of the few-reference dissociation process described above. In contrast to conventional ADC(3), SF-ADC(3) reproduces the FCI reference curves over the whole dissociation process qualitatively accurate. In the vicinity of the equilibrium

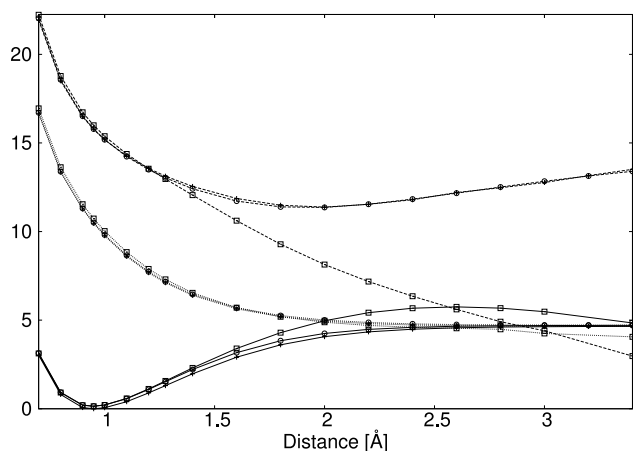


FIG. 4. Comparison of the potential energy curves of the $X^1\Sigma^+$ (solid lines), $1^1\Pi$ (dotted lines), and $2^1\Sigma^+$ (dashed lines) states of HF computed at the theoretical levels of ADC(3) (squares), SF-ADC(3) (circles), and FCI (crosses). The energy of the ground state equilibrium structure is set to zero for all three methods.

geometry, ADC(3) and SF-ADC(3) yield very similar curves, which start to deviate with increasing multi-reference character of the underlying singlet reference state. While ADC(3) breaks down, SF-ADC(3) remains stable in qualitative agreement with the FCI reference.

In summary, for single-bond dissociation of H_2 and HF, all SF-ADC approaches showed a significant improvement over the standard ADC approaches. While conventional ADC(2) and ADC(3) methods are applicable in the vicinity of the equilibrium geometry, for which the singlet ground state is well described by a single reference, SF-ADC(2) and SF-ADC(3) give qualitatively correct dissociation curves over the whole dissociation process of single bonds, because the ground-state triplet reference corresponds everywhere to a single-reference. In particular, SF-ADC(3) reaches a good qualitative agreement with the FCI reference; however, the quantitative accuracy of MR-CI and MR-CC levels is not reached. For the dissociation of double bonds, single SF-ADC is not suited, since in this cases the triplet state exhibits itself few-reference character, since two electron pairs are broken. In such situations, double spin-flip ADC starting with the single-reference quintet ground state may be useful; however, this remains to be shown in the future.

B. Twisting double bonds—Ethylene torsion

The photo-induced isomerization of double bonds is an important process in biology and chemistry, since the most important photoswitches undergo this transformation. For example, human vision is initiated by light-induced isomerization of 9-*cis* retinal to all-*trans* retinal,^{57–59} and azobenzene finds widespread application as photoswitch in chemical research and material science.^{60,61} However, the theoretical description of this switching process is difficult, since a π -bond is broken and re-formed. Hence, methods are required which can describe both the closed-shell single-reference situation at planar π -bond geometry with dihedral angles of 0° and 180° and the few-reference situation at 90° , when the π -electrons are uncoupled, in analogy to σ -bond dissociation described above. Moreover, at 90° , concomitantly with a pyramidalization of one of the CH_2 groups, the singlet ground state becomes degenerate with the excited state forming a conical intersection, which allows for ultra-fast non-radiative decay, i.e., efficient switching.^{36,62,63}

Nowadays, it is well-known that standard single-reference methods are not applicable for the description of conical intersections with the electronic ground state due to their inherent multi-reference character.³⁵ However, it has been demonstrated recently that spin-flip approaches starting from the single-reference triplet ground state are indeed capable of describing the conical intersection within the singlet manifold physically correct.^{23,28,29,34,35,37} To investigate whether also SF-ADC methods can be employed to investigate conical intersections, the potential energy curves along the torsional motion of the double bond of ethylene have been computed. For that objective, the ground state geometry of ethylene has been optimized at the theoretical level of CCSD/6-31G resulting in bond lengths of the C–C bond and the C–H bonds of 1.343 Å and 1.089 Å, respectively, and a H–C–H angle of

117.8°. The twisting angle has been scanned without relaxation of the other coordinates.

Let us first start with the ground state potential energy surface along this path. As reference method, CASSCF in combination with multi-reference singles plus doubles configuration interaction in combination with the Pople correction (MR-SDCI+Q) as implemented into the COLUMBUS program package (version 7.0) has been used.⁶⁴ In analogy to Ref. 65, the MRCI calculation was performed based on an extended restricted active reference space. In detail, first a CASSCF(2,2) has been performed, followed by a MR-SDCI calculation using the same reference space. Then, the resulting natural orbitals of the ground state have been used and a large-scale MR-SDCI+Q calculation has been done within the CAS space augmented by five σ and σ^* orbitals, with additional double excitations in this space. Following this procedure, an improved description is realized, since quadruply excited configurations are included. The unrelaxed scan of the ground state potential energy surface at this level of theory is depicted together with other methods in Figure 5. It can be seen that the conical intersection is missed along this scan, because the CH₂ groups remain planar and are not allowed to pyramidalize, resulting in an energy barrier for this rotation of about 3.2 eV.

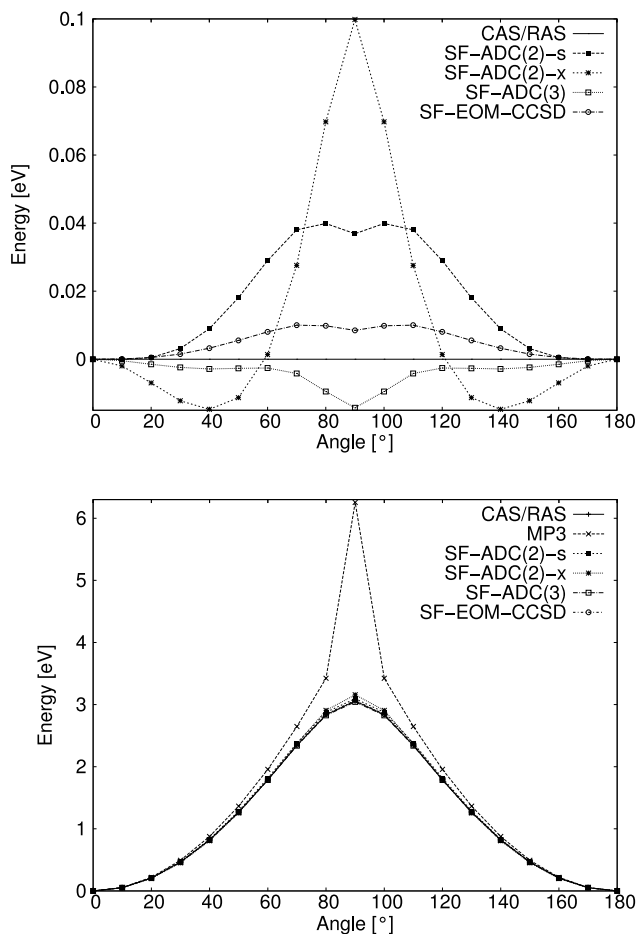


FIG. 5. Calculated potential energy curves of the electronic ground state of ethylene along the unrelaxed twisting motion (top). Absolute errors of the spin-flip methods along the twisting motion of ethylene compared to the CASSCF/MRCI benchmark curve (bottom). The energy of the planar ethylene structure is set to zero for all curves.

While MP3 gives a qualitatively wrong picture of the barrier, with an enormously too large height, due to the breakdown of the single-reference nature of the singlet ground state in the vicinity of the conical interaction, all applied spin-flip methods yield qualitatively correct potential energy curves with comparably small deviations from the CASSCF/MRCI barrier height (Figure 5). SF-ADC(2)-x exhibits the largest absolute error of 0.1 eV, while SF-ADC(2)-s performs slightly better overestimating the barrier height by only 0.04 eV. SF-ADC(3) and SF-EOM-CCSD exhibit similar errors in opposite directions, the first underestimating the barrier height by 0.015 eV and the latter overestimating it by 0.01 eV.

In addition to only investigating the ground state potential curve along the torsion of ethylene, also the excited states have been calculated at SF-ADC level. In Figure 6, the corresponding potential energy curves of S_0 , S_1 , and S_2 computed at SF-ADC(3) level are displayed. The SF-ADC(2) methods yield a qualitatively equivalent picture, which is in excellent agreement with previously published potential energy curves at multi-reference multi-state CASPT2 level.³⁶ In contrast to the conventional ADC methods, it becomes evident from this initial test that SF-ADC methods, and in particular SF-ADC(3), are capable of describing potential energy surfaces in the vicinity of conical intersections with the electronic ground state involving double bond torsion. In the future, this will be further explored when nuclear excited state gradients are available. Then, conical intersections can be directly optimized using the spin-flip ADC methodology outlined above.

C. Excited states of square-planar and rectangular cyclobutadiene

CBD is a famous example and often exploited as test case for molecules with diradicaloid character, or in other words, for molecules with multi-reference ground states.^{38,39} In the singlet 1A_g ground state CBD has a rectangular geometry with D_{2h} symmetry and is known to undergo an automerization reaction between two symmetry equivalent minima via a square planar transition state with D_{4h} symmetry.^{38,39}

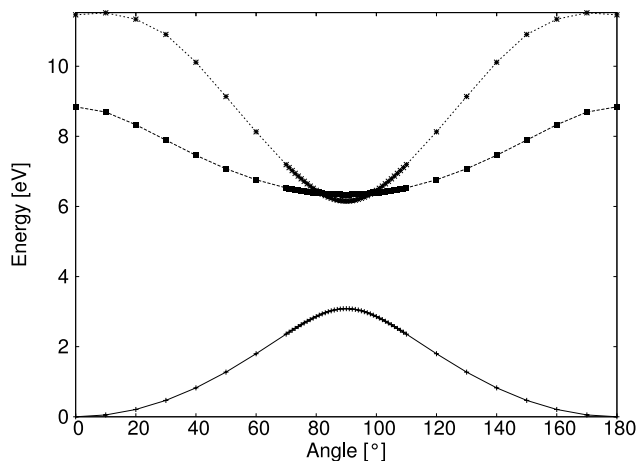


FIG. 6. Unrelaxed potential energy curves of the S_0 (solid line), S_1 (dashed line), and S_2 (dotted line) along the ethylene torsion at the level of SF-ADC(3)/6-31G. The energy of the planar equilibrium geometry is set to zero. The conical intersection is indicated.

In the D_{2h} symmetric geometries, the highest occupied and lowest unoccupied molecular orbitals (HOMO and LUMO) are non degenerate, which result in doubly occupied orbitals only and essentially single-reference character. Thus, conventional single-reference methods are applicable.³⁹ However, at the square planar geometry, HOMO and LUMO are exactly degenerate, leading to two essentially singly occupied orbitals and pronounced multi-reference character of the singlet state, such that conventional single-reference methods fail. At D_{4h} symmetry, the singlet electronic ground state assumes $^1B_{1g}$ symmetry. Not surprisingly, the corresponding triplet configuration at D_{4h} symmetry corresponds to the lowest triplet state of CBD with $^3A_{2g}$ symmetry, which is a true single-reference state. In fact, the equilibrium structure of the triplet $^3A_{2g}$ ground state is square planar with D_{4h} symmetry. Due to this electronic structure of CBD and the interplay of triplet and singlet states along the automerization coordinate, it represents an ideal testing ground for spin-flip approaches. For our test calculations, the CCSD(T)/cc-pVTZ optimized equilibrium structures of CBD of the singlet 1A_g ground state with D_{2h} symmetry as well as the equilibrium structure of the triplet $^3A_{2g}$ state with D_{4h} symmetry have been used and were taken from the literature³⁸ (Fig. 7).

As a first test, the excitation energies of CBD have been calculated at the D_{2h} symmetric equilibrium structure of the singlet ground state exhibiting a closed-shell electronic configuration using our new SF-ADC methods in combination with the cc-pVTZ basis set and compared to existing SF-EOM-CC values (Table I). At the most accurate levels of CC theory, i.e., EOM-SF-CCSD(fT) and EOM-SF-CCSD(dT) in combination with a restricted-open shell Hartree-Fock (ROHF) reference yield excitation energies of 1.515 eV, 3.256 eV, and 4.200 eV as well as 1.468 eV, 3.205 eV, and 4.170 eV for the excitation energies of the 1^3B_{1g} , 1^1B_{1g} , and 2^1A_{1g} states, respectively. At the most accurate ADC level, i.e., SF-ADC(3), these states exhibit very similar values of 1.456 eV, 3.285 eV, and 4.334 eV, when an unrestricted Hartree-Fock reference is employed. In case a restricted open-shell Hartree-Fock reference is used, the excitation energies decrease slightly by at most 0.03 eV at SF-ADC(3) level and values of 1.453 eV, 3.276 eV, and 4.302 eV are obtained for the 1^3B_{1g} , 1^1B_{1g} , and 2^1A_{1g} states, respectively. Also, SF-ADC(2)-s and SF-ADC(2)-x yield values of the excitation energies of these states which are in good agreement with the higher-levels of theory, as the deviations are in the order of 0.3 eV or less and the order of the states is strictly conserved. It is worthwhile to note that the excitation energies of the SF-ADC methods are practically not influenced by the choice of an UHF or ROHF reference.

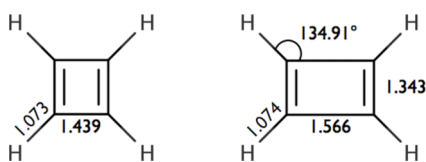


FIG. 7. Geometrical parameters of the D_{4h} equilibrium structure of the triplet $^3A_{2g}$ ground state (left) and the D_{2h} symmetric equilibrium structure of the singlet 1A_g ground state (right) at the level of CCSD(T)/cc-pVTZ.³⁸ Bond lengths are given in Å.

TABLE I. Total energy of the singlet 1A_g ground state and vertical excitation energies of the $^3B_{1g}$, $^1B_{1g}$, and $^1A_{1g}$ states at the D_{2h} symmetric equilibrium structure of the singlet ground state using spin-flip CC and ADC methods. Total energies are given in hartree and excitation energies in eV.

Method	E_{tot} (X^1A_g)	1^3B_{1g}	1^1B_{1g}	2^1A_{1g}
EOM-SF-CCSD ^{a,b}	-154.424 96	1.654	3.416	4.360
EOM-SF-CCSD(fT) ^{a,b}	-154.429 70	1.516	3.260	4.205
EOM-SF-CCSD(dT) ^{a,b}	-154.429 69	1.475	3.215	4.176
EOM-SF-CCSD ^{a,c}	-154.425 45	1.656	3.412	4.354
EOM-SF-CCSD(fT) ^{a,c}	-154.429 76	1.515	3.256	4.200
EOM-SF-CCSD(dT) ^{a,c}	-154.429 57	1.468	3.205	4.170
SF-ADC(2)-s ^b	-154.389 01	1.573	3.208	4.247
SF-ADC(2)-x ^b	-154.415 83	1.576	3.141	3.796
SF-ADC(3) ^b	-154.424 73	1.456	3.285	4.334
SF-ADC(2)-s ^c	-154.398 36	1.569	3.203	4.237
SF-ADC(2)-x ^c	-154.424 77	1.569	3.139	3.791
SF-ADC(3) ^c	-154.432 89	1.453	3.276	4.302

^aFrom Ref. 38.

^bUHF reference.

^cROHF reference.

As a further test of the applicability of SF-ADC, the vertical excited singlet states of CBD have been calculated for the singlet ground state at the D_{4h} symmetric equilibrium structure of the triplet $^3A_{2g}$ state. As mentioned above, at this structure, the multi-reference character is more pronounced than at the previously investigated D_{2h} structure. The results of previous SF-EOM-CC and our new SF-ADC calculations are compiled in Table II. At the most accurate EOM-SF-CCSD(dT) level, independent of whether an unrestricted or a restricted open-shell HF reference is employed, very similar excitation energies are obtained for the 1^3A_{2g} , 2^1A_{1g} , and 1^1B_{2g} states. With the unrestricted HF reference, they amount to 0.098 eV, 1.456 eV, and 1.853 eV, with a ROHF reference to 0.088 eV, 1.438 eV, and 1.837 eV, respectively. The results of our SF-ADC(3) calculations agree very well with these CC results, as they give values of 0.083 eV, 1.621 eV, and 1.930 eV in combination with a UHF reference and 0.075 eV, 1.607 eV, and

TABLE II. Total energy of the $^1B_{1g}$ ground state and vertical excitation energies of the $^3A_{2g}$, 2^1A_{1g} , and 1^1B_{2g} states at the square-planar equilibrium structure of the $^3A_{2g}$ state. Total energies are given in hartree and excitation energies in eV.

Method	E_{tot} (X^1B_{1g})	1^3A_{2g}	2^1A_{1g}	1^1B_{2g}
EOM-SF-CCSD ^{a,b}	-154.413 01	0.369	1.824	2.143
EOM-SF-CCSD(fT) ^{a,b}	-154.414 78	0.163	1.530	1.921
EOM-SF-CCSD(dT) ^{a,b}	-154.413 90	0.098	1.456	1.853
EOM-SF-CCSD ^{a,c}	-154.413 42	0.369	1.814	2.137
EOM-SF-CCSD(fT) ^{a,c}	-154.414 77	0.159	1.521	1.915
EOM-SF-CCSD(dT) ^{a,c}	-154.413 58	0.088	1.438	1.837
SF-ADC(2)-s ^b	-154.375 42	0.266	1.664	1.910
SF-ADC(2)-x ^b	-154.399 33	0.217	1.123	1.799
SF-ADC(3) ^b	-154.409 46	0.083	1.621	1.930
SF-ADC(2)-s ^c	-154.384 46	0.262	1.651	1.905
SF-ADC(2)-x ^c	-154.408 18	0.215	1.128	1.801
SF-ADC(3) ^c	-154.417 35	0.075	1.607	1.915

^aFrom Ref. 38.

^bUHF reference.

^cROHF reference.

1.915 eV with a ROHF reference for these states. The second order SF-ADC methods deviate slightly more, in particular, the excitation energy of the 1^3A_{2g} state is larger with values between 0.21 and 0.27 eV, which is also the case for the lower-order SF-CC schemes. While ADC(2)-s gives similar values as SF-ADC(3) for the other two 2^1A_{1g} and 1^1B_{2g} states, SF-ADC(2)-x tends to underestimate them slightly.

Summarizing the results of the excited state calculations for cyclobutadiene, SF-ADC(3) provides as accurate results as SF-EOM-CCSD(T) schemes and represents thus a valuable alternative. In particular, because the computational effort of ADC(3) scales only with $O(N^6)$, with N being the number of basis functions, while EOM-CCSD(T) scales with $O(N^7)$. The second-order SF-ADC(2) methods yield qualitatively correct results with deviations of 0.2-0.3 eV compared to the higher-level values; however, SF-ADC(2)-x tends to underestimate excitation energies as it has already been observed for the conventional method as well.⁴⁵

A challenging reaction for electronic-structure theory is the automerization reaction of cyclobutadiene in the singlet ground state, since the reaction proceeds from one D_{2h} symmetric minimum via the D_{4h} symmetric transition state to a second symmetry equivalent D_{2h} with alternated bond orders. Along this path, the multi-reference character of the state changes, and hence, the computation of the reaction barrier requires a balanced description of mostly single-reference and mostly multi-reference situations. Not only the computation of this energy barrier is difficult but also its experimental determination, as measured experimental values range between 1.6 and 10 kcal/mol.^{69,70}

In Table III, previously computed theoretical values for the automerization energy barrier of cyclobutadiene are compiled and compared to values obtained using the SF-ADC methods. In general, the ΔE values are calculated as energy difference between the D_{4h} transition state and the D_{2h} minima, $\Delta E = E_{D_{4h}} - E_{D_{2h}}$. In our calculations of the barrier at SF-ADC level, the optimized structure of the 1^3B_{1g} state is employed to approximate the transition state (Figure 7). It is clear that the computed values are thus upper bounds, since an optimization of the transition state would slightly lower the barrier. However, the equilibrium structure of the 3^3B_{1g} state and one of the transition states of the singlet ground state can be expected to be very similar due to their strongly related electronic structures.

The computed barrier heights at the SF-ADC levels lie in the range between 8.5 and 10.4 kcal/mol (Table III). These values agree very well with the values computed at EOM-SF-CC and MR-CC levels as they span the same range and the average of all reported CC values is 8.62 kcal/mol. By comparison of the values obtained at the different SF-ADC levels, it becomes apparent that the obtained values are practically independent of the employed reference. For example, the barrier height has values of 9.6 kcal/mol and 9.8 kcal/mol at SF-ADC(3) level when a UHF or a ROHF reference is employed, respectively. In summary, SF-ADC methods are also capable of describing the automerization reaction of cyclobutadiene qualitatively correct with a good quantitative accuracy. Keeping the reduced computational effort compared to true MR-CC and MR-CI methods in mind, SF-ADC methods are

TABLE III. Computed barrier heights of the automerization reaction of cyclobutadiene at various levels of theory given in kcal/mol.

Method	ΔE
EOM-SF-CCSD ^{a,b}	7.5
EOM-SF-CCSD(rT) ^{a,b}	9.4
EOM-SF-CCSD(dT) ^{a,b}	9.9
EOM-SF-CCSD ^{a,c}	7.5
EOM-SF-CCSD(rT) ^{a,c}	9.4
EOM-SF-CCSD(dT) ^{a,c}	10.0
SF-ADC(2)-s ^b	8.5
SF-ADC(2)-x ^b	10.4
SF-ADC(3) ^b	9.6
SF-ADC(2)-s ^c	8.7
SF-ADC(2)-x ^c	10.4
SF-ADC(3) ^c	9.8
UNO-MRCCSD [Mk] ^e	8.6
DNO-MRCCSD [Mk] ^e	8.6
MRCCSD [Mk] ^{c,f}	9.6
MRCCSD [Mk] ^{g,h}	9.6
CNO-MRCCSD [Mk] ^e	9.7
ULO-MRCCSD [Mk] ^e	7.1
DLO-MRCCSD [Mk] ^e	7.2
MR-CCSD(T) ⁱ	6.4
MR-CISD+Q/SS-CASSCF ^d	8.8
Expt. ^{j,k}	1.6-10

^aFrom Ref. 38.

^bUHF reference.

^cROHF reference.

^dFrom Ref. 71.

^eFrom Ref. 70.

^fFrom Ref. 66.

^gRHF reference.

^hFrom Ref. 67.

ⁱFrom Ref. 39.

^jFrom Ref. 68.

^kFrom Ref. 69.

efficient, almost black-box approaches for such few-reference situations not requiring any choice of active spaces or reference configurations, as long as the triplet ground state has single-reference character.

IV. BRIEF SUMMARY

SF-ADC schemes for the polarization propagator up to third order perturbation theory have been derived via the intermediate state representation and implemented into a development version of the Q-Chem 4.2 program package. These SF-ADC methods, i.e., SF-ADC(2)-s, SF-ADC(2)-x, and SF-ADC(3), were tested using prototypical examples with well-known multi-reference ground state character, which comprise single bond dissociation, double bond torsion, and the excited states and automerization barrier of cyclobutadiene.

As examples for single bond dissociation, the potential energy curves along the dissociation of H_2 and HF have been computed using SF-ADC and compared to the corresponding SF-EOM-CCSD and full CI curves. In contrast to conventional ADC methods, all spin-flip ADC methods give qualitatively correct ground state potential energy curves with NPE errors of 40–10 mhartree depending in the ADC level. While SF-ADC(2)-s exhibits the largest deviations from the FCI

reference, SF-ADC(3) agrees reasonably. A comparison of conventional ADC(3) and SF-ADC(3) with FCI in the computation of the lowest excited singlet states of HF revealed that ADC(3) is applicable in the vicinity of the equilibrium geometry; however, SF-ADC(3) is required to obtain a qualitatively correct picture over the complete dissociation process.

Similar results are found for the potential energy curves along the torsional motion of ethylene. All SF-ADC schemes as well as SF-EOM-CC methods deliver ground state potential curves along this motion, which are in agreement with the CASSCF/MRCI reference curve. In this case, SF-ADC(2)-x exhibits the largest error in the computed energy barrier height with 0.1 eV. In contrast, SF-ADC(3) underestimates the barrier by only -0.015 eV, SF-EOM-CCSD overestimates it by only 0.01 eV.

For further testing, the vertical excited states of cyclobutadiene have been calculated at the D_{2h} symmetric equilibrium geometry of the singlet $^1A_{1g}$ ground state and at the D_{4h} symmetric equilibrium structure of the triplet $^3A_{1g}$ ground state. Again, the vertical excited states computed at the SF-ADC levels agree very nicely with reference EOM-CC values. SF-ADC(2)-s and SF-ADC(2)-x values for the excitation energies are comparable to the ones obtained at EOM-SF-CCSD and EOM-SF-CCSD(fT) levels, while SF-ADC(3) excitation energies agree with those given by the EOM-SF-CCSD(dT) method. The results of both SF-ADC and SF-EOM-CC schemes are not sensitive to the choice of open-shell reference, i.e., whether an unrestricted Hartree-Fock or a restricted open-shell Hartree-Fock is employed. Also, the height of the automerization barrier of cyclobutadiene is nicely reproduced by the SF-ADC methods, as its values agree well with reference values obtained at MR-CC and SF-EOM-CC levels. In view of the computational efficiency of ADC methods in general, the SF-ADC approaches are easy-to-use, almost black-box, and reliable methods for the calculation of “few-reference” systems, as long as they possess a stable single-reference triplet ground state. In the future, the performance of SF-ADC methods in the optimization of conical intersections and in the calculation of molecular properties of molecules with few-reference ground states is going to be investigated.

ACKNOWLEDGMENTS

Daniel Lefrancois acknowledges support by the Heidelberg Graduate School “Mathematical and Computational Methods for the Sciences” and helpful discussions with Dirk R. Rehn and Dr. Felix Plasser.

¹A. Szabo and N. S. Ostlund, *Modern Quantum Chemistry: Introduction to Advanced Electronic Structure Theory* (Dover, New York, 1996).

²T. Helgaker, P. Jørgensen, and J. Olsen, *Modern Electronic-Structure Theory* (Wiley, Chichester, 2000).

³D. Cremer, *WIREs: Comput. Mol. Sci.* **1**, 509–530 (2011).

⁴R. J. Bartlett, *WIREs: Comput. Mol. Sci.* **2**, 126–138 (2012).

⁵M. W. Schmidt and M. S. Gordon, *Annu. Rev. Phys. Chem.* **49**, 233–266 (1998).

⁶J. Olsen, *Int. J. Quantum Chem.* **111**, 3267–3272 (2011).

⁷M. J. Bearpark, F. Ogliaro, T. Vreven, M. Boggio-Pasqua, M. J. Frisch, S. M. Larkin, M. Morrison, and M. A. Robb, *J. Photochem. Photobiol., A* **190**, 207–227 (2007).

⁸P. A. Malmqvist, A. Rendell, and B. O. Roos, *J. Phys. Chem.* **94**, 5477–5482 (1990).

⁹J. Finley, P. A. Malmqvist, B. O. Roos, and L. Serrano-Andres, *Chem. Phys. Lett.* **288**, 299–306 (1998).

¹⁰G. Ghigo, B. O. Roos, and P. A. Malmqvist, *Chem. Phys. Lett.* **396**, 142–149 (2004).

¹¹H.-J. Werner and P. J. Knowles, *J. Chem. Phys.* **89**, 5803 (1988).

¹²P. G. Szalay, T. Möller, G. Gidofalvi, H. Lischka, and R. Shepard, *Chem. Rev.* **112**, 108–181 (2012).

¹³A. Köhn, M. Hanauer, L. A. Mück, T.-C. Jagau, and J. Gauss, *WIREs: Comput. Mol. Sci.* **3**, 176–197 (2013).

¹⁴A. Berning, M. Schweizer, H.-J. Werner, P. J. Knowles, and P. Palmieri, *Mol. Phys.* **98**, 1823–1833 (2000).

¹⁵P. G. Szalay and R. J. Bartlett, *J. Chem. Phys.* **103**, 3600–3612 (1995).

¹⁶H. Lischka, R. Shepard, F. B. Brown, and I. Shavitt, *Int. J. Quantum Chem.* **20**, 91–100 (1981).

¹⁷M. J. S. Dewar, E. G. Zoebisch, E. F. Healy, and J. J. P. Stewart, *J. Am. Chem. Soc.* **107**, 3902–3909 (1985).

¹⁸G. G. Ferenczy, C. A. Reynolds, and W. G. Richards, *J. Comput. Chem.* **11**, 159–169 (1990).

¹⁹M. R. Silva-Junior and W. Thiel, *J. Chem. Theory Comput.* **6**, 1546–1564 (2010).

²⁰W. Weber and W. Thiel, *Theor. Chem. Acc.* **103**, 495–506 (2000).

²¹T. Ukai, K. Nakata, S. Yamanaka, T. Kubo, Y. Morita, T. Takada, and K. Yamaguchi, *Polyhedron* **26**, 2313–2319 (2007).

²²K. Sharkas, A. Savin, H. J. A. Jensen, and J. Toulouse, *J. Chem. Phys.* **137**, 044104 (2012).

²³A. I. Krylov, *Chem. Phys. Lett.* **338**, 375–384 (2001).

²⁴D. Casanova, L. V. Slipchenko, A. I. Krylov, and M. Head-Gordon, *J. Chem. Phys.* **130**, 044103 (2009).

²⁵F. Wang and T. Ziegler, *J. Chem. Phys.* **122**, 074109 (2005).

²⁶F. Wang and T. Ziegler, *J. Chem. Phys.* **121**, 12191–12196 (2004).

²⁷Y. A. Bernard, Y. Shao, and A. I. Krylov, *J. Chem. Phys.* **136**, 204103 (2012).

²⁸A. Krylov, *Chem. Phys. Lett.* **350**, 522–530 (2001).

²⁹J. S. Sears, C. D. Sherrill, and A. I. Krylov, *J. Chem. Phys.* **118**, 9084–9094 (2003).

³⁰D. Casanova and M. Head-Gordon, *J. Chem. Phys.* **129**, 064104 (2008).

³¹A. Dreuw and M. Head-Gordon, *J. Am. Chem. Soc.* **126**, 4007–4016 (2004).

³²J. Schirmer and F. Mertins, *Theor. Chem. Acc.* **125**, 145–172 (2010).

³³H. Koch, R. Kobayashi, A. Sanchez de Meras, and P. Jørgensen, *J. Chem. Phys.* **100**, 4393–4400 (1994).

³⁴A. I. Krylov and C. D. Sherrill, *J. Chem. Phys.* **116**, 3194–3203 (2002).

³⁵A. I. Krylov, *J. Chem. Phys.* **113**, 6052–6062 (2000).

³⁶R. Krawczyk, A. Viel, U. Manthe, and W. Domcke, *J. Chem. Phys.* **119**, 1397–1411 (2003).

³⁷A. I. Krylov, *Acc. Chem. Res.* **39**, 83–91 (2006).

³⁸P. U. Manohar and A. I. Krylov, *J. Chem. Phys.* **129**, 194105 (2008).

³⁹A. Balkov and R. J. Bartlett, *J. Chem. Phys.* **101**, 8972 (1994).

⁴⁰J. Schirmer, *Phys. Rev. A* **26**, 2395–2416 (1982).

⁴¹B. A. Trofimov and J. Schirmer, *J. Phys. B: At., Mol. Opt. Phys.* **28**, 2299 (1995).

⁴²A. Dreuw and M. Wormit, *WIREs: Comput. Mol. Sci.* **5**, 82 (2014).

⁴³J. Schirmer and A. B. Trofimov, *J. Chem. Phys.* **120**, 11449–11464 (2004).

⁴⁴M. Wormit, D. R. Rehn, P. H. Harbach, J. Wenzel, C. M. Krauter, E. Epifanovsky, and A. Dreuw, *Mol. Phys.* **112**, 774–784 (2014).

⁴⁵P. H. P. Harbach, M. Wormit, and A. Dreuw, *J. Chem. Phys.* **141**, 064113 (2014).

⁴⁶J. H. Starcke, M. Wormit, and A. Dreuw, *J. Chem. Phys.* **130**, 024104 (2009).

⁴⁷M. Pernpointner, *J. Chem. Phys.* **140**, 084108 (2014).

⁴⁸C. Hättig, *Adv. Quantum Chem.* **50**, 37 (2005).

⁴⁹J. Schirmer and G. Angonoa, *J. Chem. Phys.* **91**, 1754 (1989).

⁵⁰J. Schirmer, *Phys. Rev. A* **43**, 4647–4659 (1991).

⁵¹Y. Shao, L. F. Molnar, Y. Jung, J. Kussmann, C. Ochsenfeld, S. T. Brown, A. T. Gilbert, L. V. Slipchenko, S. V. Levchenko, D. P. O’Neill, R. A. DiStasio, Jr., R. C. Lochan, T. Wang, G. J. Beran, N. A. Besley, J. M. Herbert, C. Yeh Lin, T. Van Voorhis, S. Hung Chien, A. Sodt, R. P. Steele, V. A. Rassolov, P. E. Maslen, P. P. Korambath, R. D. Adamson, B. Austin, J. Baker, E. F. C. Byrd, H. Dachsel, R. J. Doerksen, A. Dreuw, B. D. Dunietz, A. D. Dutoi, T. R. Furlani, S. R. Gwaltney, A. Heyden, S. Hirata, C.-P. Hsu, G. Kedziora, R. Z. Khalliulin, P. Klunzinger, A. M. Lee, M. S. Lee, W. Liang, I. Lotan, N. Nair, B. Peters, E. I. Proynov, P. A. Pieniazek, Y. Min Rhee, J. Ritchie, E. Rosta, C. David Sherrill, A. C. Simmonett, J. E. Subotnik, H. Lee Woodcock III, W. Zhang, A. T. Bell, A. K. Chakraborty, D. M. Chipman, F. J. Keil, A. Warshel, W. J. Hehre, H. F. Schaefer III, J. Kong, A. I. Krylov,

- P. M. W. Gill, and M. Head-Gordon, *Phys. Chem. Chem. Phys.* **8**, 3172–3191 (2006).
- ⁵²F. Neese, *WIREs: Comput. Mol. Sci.* **2**, 73–78 (2012).
- ⁵³A. Engels-Putzka and M. Hanrath, *J. Mol. Struct.: THEOCHEM* **902**, 59–65 (2009).
- ⁵⁴S. Das, D. Mukherjee, and M. Kallay, *J. Chem. Phys.* **132**, 074103 (2010).
- ⁵⁵S. A. Evangelista and J. Gauss, *J. Chem. Phys.* **134**, 114102 (2011).
- ⁵⁶Ch. Li and S. A. Evangelista, *J. Chem. Theory Comput.* **11**, 2097–2108 (2015).
- ⁵⁷F. Gai, K. C. Hasson, J. C. McDonald, and P. A. Anfinrud, *Science* **279**, 1886–1891 (1998).
- ⁵⁸M. O. Lenz, R. Huber, B. Schmidt, P. Gilch, R. Kalmbach, M. Engelhard, and J. Wachtveitl, *Biophys. J.* **91**, 255–262 (2006).
- ⁵⁹K. Hasson, F. Gai, and P. Anfinrud, *Proc. Natl. Acad. Sci. U. S. A.* **93**, 15124–15129 (1996).
- ⁶⁰G. S. Kumar and D. C. Neckers, *Chem. Rev.* **89**, 1915–1925 (1989).
- ⁶¹H. Rau, *Photoisomerization of Azobenzenes* (CRC Press, Boca Raton, FL, 1990), Vol. 2.
- ⁶²M. Ben-Nun and T. J. Martinez, *Chem. Phys.* **259**, 237–248 (2000).
- ⁶³M. Barbatti, J. Paier, and H. Lischka, *J. Chem. Phys.* **121**, 11614–11624 (2004).
- ⁶⁴H. Lischka, R. Shepard, I. Shavitt, R. M. Pitzer, M. Dallos, T. Mueller, P. G. Szalay, F. B. Brown, R. Ahlrichs, H. J. Boehm, A. Chang, D. C. Comeau, R. Gdanitz, H. Dachsel, C. Ehrhardt, M. Ernzerhof, P. Hoeschl, S. Irl, G. Kedziora, T. Kovar, V. Parasuk, M. J. M. Pepper, P. Scharf, H. Schiffer, M. Schindler, M. Schueler, M. Seth, E. A. Stahlberg, J.-G. Zhao, S. Yabushita, Z. Zhang, M. Barbatti, S. Matsika, M. Schuurmann, D. R. Yarkony, S. R. Brozell, E. V. Beck, J.-P. Blaudeau, M. Ruckebauer, B. Sellner, F. Plasser, and J. J. Szyczak, COLUMBUS, an *ab initio* electronic structure program, 2011.
- ⁶⁵F. Plasser, H. Pasalic, M. H. Gerzabek, F. Libisch, R. Reiter, J. Burgdörfer, T. Müller, R. Shepard, and H. Lischka, *Angew. Chem., Int. Ed.* **52**, 2581–2584 (2013).
- ⁶⁶K. Bhaskaran-Nair, O. Demel, and J. Pittner, *J. Chem. Phys.* **129**, 184105 (2008).
- ⁶⁷X. Li and J. Paldus, *J. Chem. Phys.* **131**, 114103 (2009).
- ⁶⁸D. Whitman and B. Carpenter, *J. Am. Chem. Soc.* **104**, 6473 (1982).
- ⁶⁹B. Carpender, *J. Am. Chem. Soc.* **105**, 1700–1701 (1983).
- ⁷⁰T. Saito, S. Nishihara, Y. Kitagawa, T. Kawakami, S. Yamanaka, M. Okumura, and K. Yamaguchi, *Chem. Phys. Lett.* **498**, 253 (2010).
- ⁷¹M. Eckert-Maksi, M. Vazdar, M. Barbatti, H. Lischka, and Z. B. Maksi, *J. Chem. Phys.* **125**, 164323 (2006).